

High-spin states and band structures in ^{182}Pt

D. G. Popescu,* J. C. Waddington, J. A. Cameron, J. K. Johansson,† and N. C. Schmeing
Department of Physics and Astronomy, McMaster University, Hamilton, Ontario, Canada L8S 4K1

W. Schmitz,‡ M. P. Carpenter,§ V. P. Janzen,|| J. Nyberg,¶ and L. L. Riedinger
Department of Physics and Astronomy, University of Tennessee, Knoxville, Tennessee 37996-1200

H. Hübel
Institut für Strahlen- und Kernphysik, Universität Bonn, Nussallee 14-16, D-53115 Bonn 1, Germany

G. Kajrys, S. Monaro, and S. Pilotte**
Laboratoire de Physique Subatomique, Université de Montréal, Montréal, P.Q., Canada H3C 3J7

C. Bourgeois, N. Perrin, H. Sergolle, D. Hojman, and A. Korichi
Institut de Physique Nucléaire, 91406 - Orsay, France

(Received 3 May 1996)

Excited states in ^{182}Pt have been studied via the heavy-ion reactions $^{170}\text{Yb}(^{16}\text{O},4n)$, $^{162}\text{Dy}(^{24}\text{Mg},4n)$, and $^{163}\text{Dy}(^{24}\text{Mg},5n)$. γ -ray coincidence measurements were performed with arrays of HPGe detectors at the McMaster University Tandem Accelerator Laboratory (^{16}O -induced reaction) and the Institut de Physique Nucléaire, Orsay (^{24}Mg -induced reactions). The ground-state rotational band has been extended to $I=26\hbar$, and six new band structures have been identified and assigned quasiparticle configurations. The γ -vibrational band and the band built upon the first excited 0^+ state have also been extended. Properties of the rotational bands are compared with cranked-shell-model and total-Routhian-surface calculations. Evidence concerning shape coexistence at low spin and band crossings at high spin is discussed. [S0556-2813(97)00702-4]

PACS number(s): 21.10.Re, 23.20.Lv, 27.70+q

I. INTRODUCTION

The Pt isotopes have four protons fewer than $Z=82$, the “magic” proton number at which there is a large shell-energy gap for spherical nuclei. This difference in proton number is sufficiently large that collective correlations can establish deformation, along with associated rotational band structures, yet small enough that the properties of excited states are clearly influenced by the presence of the shell gap. This influence is particularly strong for states of low excitation energy and spin, which have been the object of much experimental and theoretical investigation for this reason (e.g., Refs. [1–3]). A picture has emerged which character-

izes the “normal” states in this region as multi-proton-hole (nh , $n=82-Z$) configurations with respect to the $Z=82$ Pb closed core, while the possibility of exciting two protons across the shell gap leads to “intruder” states in the same nucleus with a proton two-particle-multi-hole [$2p-(n+2)h$] configuration [1]. Although this may be an oversimplification, especially the farther one moves from the $Z=82$ closed shell, theoretical calculations and experimental observations support such a picture in general and for the Pt chain suggest that the “normal” states are associated with oblate deformation ($\beta_2 \approx -0.15$), the “intruder” states with prolate deformation ($\beta_2 \approx 0.25$) [4,5]. Theory also predicts coexisting band structures built upon these states, with strong mixing occurring at low spin. The $N=104$ nucleus ^{182}Pt is particularly interesting in this regard, since it lies directly in the middle of the neutron $N=82-126$ major shell. It has been suggested that neutron-proton correlations are crucial to the deformed intruder configurations becoming energetically favored and that they are maximized at this neutron number [6].

For nuclei in the vicinity of ^{182}Pt , rotational bands associated with the well-deformed prolate structures comprise the vast majority of known yrast and near-yrast states above spin $I \approx 8\hbar$ [7–16]. According to calculation, though, some influence of the oblate structures is preserved, as a degree of softness in the calculated energy surfaces. This leads to the possibility of dynamic effects, such as γ and β vibrations, and shape changes caused by the occupation of deformation-driving orbitals which lie near the Fermi surface, such as the high- j $\nu i_{13/2}$, $\pi h_{9/2}$, and $\pi i_{13/2}$ orbitals. Occupying the

*Present address: Institut de Physique Nucléaire, 91406 - Orsay, France.

†Present address: Ontario Hydro Research, 800 Kipling Ave., Toronto, ON, Canada M8Z 5S4.

‡On leave from Institut für Strahlen- und Kernphysik, Universität Bonn, Nussallee 14-16, D-53115 Bonn 1, Germany.

§Present address: Argonne National Laboratory, Physics Division, 9700 Cass Avenue, Argonne, IL 60439.

||Present address: AECL, Chalk River Laboratories, Chalk River, ON, Canada K0J 1J0.

¶Present address: The Svedberg Laboratory, Box 533, S-75121 Uppsala, Sweden.

**Present address: Centre de Recherches Nucléaires, IN2P3-CRNS/Université Louis Pasteur, F-67037 Strasbourg Cedex, France.

$\nu i_{13/2}$ orbital, whether as one component of a two-quasiparticle excited band or as a broken pair following rotational alignment, is expected to induce a change toward negative γ deformation, whereas occupying either the $\pi h_{9/2}$ or the $\pi i_{13/2}$ orbital is expected to lead to an enhancement in the quadrupole deformation β_2 and also a change toward positive γ deformation. There is also some question as to which rotational band crossings occur in the light Pt and nearby nuclei, with the possibilities of a pair of $i_{13/2}$ neutrons and/or a pair of $h_{9/2}$ protons being raised (e.g., [8,12]).

Although there have been many experimental studies of nuclei in this mass region, there are no published results dealing with the high-spin properties of ^{182}Pt .¹ Previous in-beam γ -ray work on this nucleus by Burde *et al.* [17], established the ground-state rotational band to spin (12^+) . The subsequent electron and γ -ray spectroscopy measurements of Cailliau *et al.* [19] and Husson *et al.* [18], who studied the β decay of ^{182}Au , revealed 0_2^+ and 2_3^+ states, which, they suggested, might represent the lowest members of a ‘‘quasi- β' ’’-vibrational band. They also observed the 2_2^+ , 3^+ , and 4_2^+ states, which they interpreted as belonging to a γ -vibrational band.

The present work outlines γ -ray spectroscopic studies following heavy-ion compound-nucleus reactions, designed to examine the properties of high-spin states in ^{182}Pt and to relate them to the existing experimental and theoretical evidence concerning shape coexistence, dynamic effects, and the characteristics of band crossings in this mass region.

II. EXPERIMENTAL DETAILS

Measurements of high-spin states in ^{182}Pt were made at two accelerator laboratories. At the McMaster University Tandem Accelerator Laboratory, an isotopically enriched (85%) target of ^{170}Yb (1.9 mg cm^{-2}) on a 5.4-mg/cm^2 backing of ^{208}Pb was bombarded by a beam of ^{16}O . An excitation function was performed and a beam energy of 95 MeV found to optimize the population of high-spin states in ^{182}Pt . An array of eight high-purity (HP) Ge detectors (each having 25% relative efficiency, with no Compton-scattering suppression) was used to detect γ rays, with six additional NaI scintillation counters acting as a multiplicity filter. Five of the HPGe detectors were located in the reaction plane at approximately 0, 30, 45, 60, and 90 degrees with respect to the beam axis and the other three in a plane perpendicular to the beam axis, with all detectors approximately 12 cm from the target. The HPGe and NaI detector faces were covered with graded Pb, Cd, and Cu shields in order to reduce the intensity of Pb x rays. In addition, the sides of the detectors were shielded with lead to prevent scattering of γ rays from one detector to another. The relative efficiencies of the detectors were determined with standard ^{152}Eu and ^{133}Ba γ -ray calibration sources.

Events consisting of either three HPGe detectors or two

HPGe detectors plus at least two NaI counters firing in prompt coincidence (within $\approx 70 \text{ ns}$) were recorded. Approximately 250×10^6 HPGe twofold coincidences were collected. These events were subsequently sorted into a 4096-channel \times 4096-channel matrix, from which the background was subtracted with the method of Palameta and Waddington [20]. Coincidence relationships between transitions were determined with standard gating techniques. Furthermore, the A_2, A_4 angular-distribution coefficients were extracted from spectra taken at each of the five detector angles in the reaction plane. For those angular distributions which indicated pure dipole character the transitions were assigned as $E1$, since the possibility of pure $M1$ radiation with no $E2$ admixture was considered highly unlikely.

A second experiment, designed to extend the bands to higher spins, was performed at the MP Tandem accelerator laboratory in Orsay with the ‘‘Chateau de Cristal’’ γ -ray spectrometer, which comprised 12 Compton-suppressed HPGe detectors, 8 of 80% and 4 of 25% relative efficiency, combined with a 38-element BaF_2 sum-energy and multiplicity filter. The $^{162,163}\text{Dy}(^{24}\text{Mg},4n)$ reactions at 129 MeV were used, the targets consisting of enriched 1.3-mg/cm^2 foils. With the requirement that at least two HPGe detectors and four BaF_2 detectors fired, approximately 80×10^6 two-and-higher-fold events were obtained. The data were analyzed with standard coincidence gating and background-subtraction techniques.

III. EXPERIMENTAL RESULTS

A decay scheme for ^{182}Pt is shown in Fig. 1 and a summary of the transition energies, relative intensities, and the results of the angular distributions measurements is presented in Table I. The decay scheme is similar to that obtained for ^{184}Pt by Carpenter *et al.* [12] and we have labeled the bands in a manner which is consistent with that study. In some instances it has not been possible to unambiguously determine spins and/or parities, although in all cases the labels in the figure are consistent with the data and agree with systematic features of the even-even nuclei in the vicinity. A brief explanation of some aspects of the decay scheme follows.

A. Yrast band 1

The ground-state band was previously known to spin (12^+) [17] and has now been extended to 26^+ . Figure 2 presents the γ -ray spectrum gated on the 634-keV member of the band. This line is clearly a doublet and a sharp drop in the intensities for the higher energy transitions is observed. It can be seen from Fig. 1 that band 1 remains yrast to the highest spins observed.

B. Band 8 and the γ band

Two short cascades have been observed. Band 8, possibly a low-deformation band (see below), consists of four stretched $E2$ transitions with higher transition energies than the yrast cascade. In addition six members of a positive-parity band have been assigned as the γ -vibrational band (γ band). The lowest-spin members of both of these bands were known previously [18].

¹During preparation of this manuscript, the unpublished data of R. Bark *et al.* [21] came to our attention. The results agree, for the most part, with the present work; some possible differences are mentioned in Sec. III.

TABLE I. Properties of γ -ray transitions placed in ^{182}Pt .

Energy ^a	$I_i \rightarrow I_f$	Bands	I_γ ^b	A_2	A_4	δ	Multipolarity
91.5	$7^- \rightarrow 6^+$	4/3	1.9(7)				
127.0	$8^- \rightarrow 7^-$	3/4	3.0(3)	-0.53(4)	-0.06(6)	0.25(15)	$M1/E2$
133 ^c	$6^+ \rightarrow 5^+$	γ					
138 ^c	$(18^+) \rightarrow 18^+$	7/1					
155.0	$2^+ \rightarrow 0^+$	1	72.1(35)				
159.3	$9^- \rightarrow 8^-$	4/3	2.0(2)	-0.53(4)	0.01(33)	-0.21(7)	$M1/E2$
185.8	$10^- \rightarrow 9^-$	3/4	3.2(3)	-0.56(6)	0.02(5)	-0.21(6)	$M1/E2$
186	$(16^+) \rightarrow 16^+$	7/1					
191	$(20^+) \rightarrow 20^+$	7/1					
207.4	$11^- \rightarrow 10^-$	4/3	2.8(3)	-0.53(7)	0.01(8)	-0.18(7)	$M1/E2$
225	$(8^-) \rightarrow 7^-$	6/5					
225.2	$12^- \rightarrow 11^-$	3/4	3.1(3)	-0.68(8)	0.02(9)	-0.29(15)	$M1/E2$
243.1	$13^- \rightarrow 12^-$	4/3	1.7(2)	-0.27(9)	0.01(9)	-0.02(5)	$M1/E2$
254.1	$7^- \rightarrow 5^-$	5	5.3(7)				
254.4	$14^- \rightarrow 13^-$	3/4	2.1(4)				
263	$(10^-) \rightarrow 9^-$	6/5					
264	$(13^-) \rightarrow 14^+$	2/1					
264.3	$4^+ \rightarrow 2^+$	1	118.9(44)	0.34(3)	-0.12(3)		$E2$
271	$5^+ \rightarrow 4^+$	γ					
271.5	$15^- \rightarrow 14^-$	4/3	2.3(6)				
275	$(7^-) \rightarrow 6^+$	5/8	3.8(3)				
276.9	$16^- \rightarrow 15^-$	3/4	2.0(2)	-0.17(9)	0.00(9)	-0.04(8)	$M1/E2$
285	$7^- \rightarrow 5^-$	3/5	3.8(4)	0.35(7)	-0.11(8)		$E2$
286.3	$9^- \rightarrow 7^-$	4	4.7(4)	0.31(5)	-0.07(6)		$E2$
296.9	$18^- \rightarrow 17^-$	3/4	2.4(7)				
297.3	$17^- \rightarrow 16^-$	4/3	2.5(7)				
304.7	$(8^-) \rightarrow (6^-)$	6	3.5(4)				
306.0	$7^- \rightarrow 6^+$	4/8	3.3(6)				
314.5	$20^- \rightarrow 19^-$	3/4					
316.1	$9^- \rightarrow 7^-$	5	11.2(7)	0.32(4)	-0.08(4)		$E2$
317	$(12^-) \rightarrow 11^-$	6/5					
324.7	$19^- \rightarrow 18^-$	4/3					
336.2	$(14^+) \rightarrow 14^+$	7/1					
345	$0^+ \rightarrow 2^+$	8/1					
345.1	$10^- \rightarrow 8^-$	3	8.9(5)	0.37(5)	-0.11(5)		$E2$
353.9	$(10^-) \rightarrow (8^-)$	6	2.3(8)				
355.0	$6^+ \rightarrow 4^+$	1	100.0(5)	0.34(3)	-0.10(3)		$E2$
356	$2^+ \rightarrow 0^+$	8					
362	$5^+ \rightarrow 3^+$	γ					
366	$4^+ \rightarrow 2^+$	γ					
374.2	$11^- \rightarrow 9^-$	5	12.2(10)	0.37(4)	-0.12(4)		$E2$
383	$4^+ \rightarrow 2^+$	8					
383.4	$(15^-) \rightarrow (13^-)$	2	3.8(4)				
393.2	$11^- \rightarrow 9^-$	4	8.8(5)	0.30(5)	-0.06(5)		$E2$
404	$6^+ \rightarrow 4^+$	γ					
407	$(13^-) \rightarrow (12^+)$	2/7					
410	$6^+ \rightarrow 4^+$	8					
419	$(8^-) \rightarrow 7^+$	6/ γ					
427	$7^+ \rightarrow 5^+$	γ					
427.4	$(12^-) \rightarrow (10^-)$	6	4.9(9)				
428	$(16^-) \rightarrow 15^-$	6/5					
430.9	$8^+ \rightarrow 6^+$	1	92.2(55)	0.31(3)	-0.07(3)		$E2$
431.2	$13^- \rightarrow 11^-$	5					
432	$5^- \rightarrow 4^+$	5/8					
432.7	$12^- \rightarrow 10^-$	3					

TABLE I (Continued).

Energy ^a	$I_i \rightarrow I_f$	Bands	I_γ ^b	A_2	A_4	δ	Multipolarity
433	$(15^-) \rightarrow 13^-$	2/5					
446	$15^- \rightarrow (13^-)$	5/2					
446	$6^+ \rightarrow 8^+$	8/1					
448	$(12^+) \rightarrow 12^+$	7/1					
464	$4^+ \rightarrow 6^+$	8/1					
468	$8^+ \rightarrow 6^+$	8					
468.4	$13^- \rightarrow 11^-$	4	9.3(8)	0.39(6)	-0.14(6)		E2
476.4	$(16^+) \rightarrow (14^+)$	7					
477	$(18^-) \rightarrow 17^-$	6/5					
478	$(14^+) \rightarrow (12^+)$	7					
487	$7^- \rightarrow 6^+$	5/ γ					
492.6	$10^+ \rightarrow 8^+$	1	72.0(45)	0.33(5)	-0.08(3)		E2
493.8	$(14^-) \rightarrow (12^-)$	6	3.1(8)				
495.6	$15^- \rightarrow 13^-$	5	4.3(8)	0.34(7)	-0.09(7)		E2
497.5	$14^- \rightarrow 12^-$	3	9.6(6)	0.29(7)	-0.05(7)		E2
502.4	$(17^-) \rightarrow (15^-)$	2	9.3(9)	0.32(9)	-0.08(9)		E2
511	$(20^-) \rightarrow (19^-)$	6/5					
512	$2^+ \rightarrow 2^+$	$\gamma/1$					
518	$7^- \rightarrow 6^+$	4/ γ					
522	$(17^-) \rightarrow 16^+$	2/1					
523	$7^+ \rightarrow 8^+$	$\gamma/1$					
525.9	$15^- \rightarrow 13^-$	4	11.3(10)	0.37(6)	-0.12(6)		E2
530	$5^+ \rightarrow 6^+$	$\gamma/1$					
535.9	$17^- \rightarrow 15^-$	5	5.7(5)	0.19(6)	-0.02(6)		E2
540	$(6^-) \rightarrow 5^+$	6/ γ	3.7(6)	-0.04(10)	0.00(10)		
543.5	$12^+ \rightarrow 10^+$	1	64.7(38)	0.20(3)	-0.10(3)		E2
546.0	$(16^-) \rightarrow (14^-)$	6	8.0(11)	0.38(8)	-0.13(9)		E2
548.4	$16^- \rightarrow 14^-$	3	8.7(8)	0.34(6)	-0.09(6)		E2
559	$6^+ \rightarrow 5^+$	-/ γ	1.9(6)	-0.10(20)	0.00(21)		
574.2	$17^- \rightarrow 15^-$	4	8.9(9)	0.32(9)	-0.08(9)		E2
579.7	$19^- \rightarrow 17^-$	5	6.4(6)	0.37(11)	-0.12(11)		E2
583.7	$(18^-) \rightarrow (16^-)$	6	3.5(5)				
587.0	$(18^+) \rightarrow (16^+)$	7					
587.2	$(19^-) \rightarrow (17^-)$	2	12.2(12)	0.37(7)	-0.13(7)		E2
590.0	$14^+ \rightarrow 12^+$	1	43.1(22)	0.38(3)	-0.13(4)		E2
594.2	$18^- \rightarrow 16^-$	3	5.3(5)	0.35(15)	-0.10(15)		E2
599	$13,14 \rightarrow (12^+)$	-/7					
611.1	$(20^-) \rightarrow (18^-)$	6	2.6(8)				
613	$4^+ \rightarrow 4^+$	$\gamma/1$	8.0(10)	-0.02(11)	0.00(9)		M1/E2
621.5	$21^- \rightarrow 19^-$	5	4.1(8)	0.20(9)	-0.02(9)		E2
621.6	$19^- \rightarrow 17^-$	4	6.7(9)	0.20(9)	-0.02(9)		E2
624	$24^- \rightarrow 22^-$	3					
628.5	$16^+ \rightarrow 14^+$	1	28.0(18)	0.38(4)	-0.13(4)		E2
633.8	$18^+ \rightarrow 16^+$	1	15.8(15)	0.37(6)	-0.13(6)		E2
634.6	$20^+ \rightarrow 18^+$	1	9.3(13)	0.26(8)	-0.04(8)		E2
636	$22^- \rightarrow 20^-$	3					
637.4	$(22^-) \rightarrow (20^-)$	6					
638.3	$(21^-) \rightarrow (19^-)$	2	8.8(6)	0.36(9)	-0.11(9)		E2
639.2	$20^- \rightarrow 18^-$	3	6.6(5)	0.36(9)	-0.11(9)		E2
648.3	$(15^-) \rightarrow 14^+$	2/1	4.8(7)	-0.11(22)	0.00(21)		
662	$6^+ \rightarrow 6^+$	$\gamma/1$					
667	$2^+ \rightarrow 0^+$	$\gamma/1$					
669.2	$21^- \rightarrow 19^-$	4	2.6(5)	0.37(31)	-0.12(31)		
673	$23^- \rightarrow 21^-$	5	3.4(5)	0.37(13)	-0.12(12)		E2
674.7	$22^+ \rightarrow 20^+$	1	5.5(5)	0.37(16)	-0.12(16)		E2

TABLE I (*Continued*).

Energy ^a	$I_i \rightarrow I_f$	Bands	I_γ ^b	A_2	A_4	δ	Multipolarity
675	(24 ⁻) \rightarrow (22 ⁻)	6					
686	(23 ⁻) \rightarrow (21 ⁻)	2					
687.0	(20 ⁺) \rightarrow (18 ⁺)	7					
699	2 ⁺ \rightarrow 2 ⁺	8/1					
714	23 ⁻ \rightarrow 21 ⁻	4	2.0(9)	0.34(8)	-0.09(8)		E2
718.6	(22 ⁺) \rightarrow (20 ⁺)	7					
719	7 ⁻ \rightarrow 8 ⁺	5/1	3.2(5)				
723.6	24 ⁺ \rightarrow 22 ⁺	1	5.2(6)	0.13(15)	-0.01(15)		
731	(25 ⁻) \rightarrow (23 ⁻)	2					
743	(24 ⁺) \rightarrow (22 ⁺)	7					
750	7 ⁻ \rightarrow 8 ⁺	4/1	2.2(4)	-0.20(8)	0.00(8)		E1
753	25 ⁻ \rightarrow 23 ⁻	4					
771.1	(18 ⁺) \rightarrow 16 ⁺	7/1					
772	(27 ⁻) \rightarrow (25 ⁻)	2					
778.0	26 ⁺ \rightarrow 24 ⁺	1	2.0(9)				
787	3 ⁺ \rightarrow 2 ⁺	γ /1					
799	27 ⁻ \rightarrow 25 ⁻	4					
812.6	(16 ⁺) \rightarrow 14 ⁺	7/1					
819	4 ⁺ \rightarrow 4 ⁺	8/1					
824.6	(20 ⁺) \rightarrow 18 ⁺	7/1					
831	6 ⁺ \rightarrow 4 ⁺	-/ γ	2.4(4)	0.36(12)	-0.11(11)		E2
854.4	(13 ⁻) \rightarrow 12 ⁺	2/1	2.9(4)				
855	2 ⁺ \rightarrow 0 ⁺	8/1					
875	6 ⁺ \rightarrow 4 ⁺	8/1					
878	4 ⁺ \rightarrow 2 ⁺	γ /1					
885	5 ⁺ \rightarrow 4 ⁺	γ /1	8.7(9)	0.42(12)	-0.29(14)		
896	5 ⁻ \rightarrow 6 ⁺	5/1					
955	7 ⁺ \rightarrow 6 ⁺	γ /1	3.0(5)	0.24(5)	-0.04(4)		E2
992	(12 ⁺) \rightarrow 10 ⁺	7/1					
1017	6 ⁺ \rightarrow 4 ⁺	γ /1					
1036	9 ⁻ \rightarrow 8 ⁺	5/1					
1048	13,14 \rightarrow 12 ⁺	-/1					
1083	4 ⁺ \rightarrow 2 ⁺	8/1	3.6(6)				
1089	6 ⁺ \rightarrow 6 ⁺	-/1	4.1(5)	0.10(10)	0.00(10)		
1149	7 ⁻ \rightarrow 6 ⁺	5/1					
1229	6 ⁺ \rightarrow 4 ⁺	8/1	4.5(5)	0.12(12)	-0.01(12)		(E2)
1250	5 ⁻ \rightarrow 4 ⁺	8/1	3.9(5)	-0.03(11)	0.00(11)		E1
1443	6 ⁺ \rightarrow 4 ⁺	-/1	2.3(6)				

^aThe uncertainty in γ -ray energies is ± 0.1 keV for transitions with $I_\gamma > 10$ and ± 1.0 keV for the remainder.

^bIntensities are normalized to 100 for the 355.0-keV 6⁺ \rightarrow 4⁺ transition. If no value is given, the transition is either too weak or contaminated and a reliable intensity measurement was not possible.

^cThese transitions were only observed in the magnesium-induced reaction.

present work, these bands have been identified up to the (24⁻) and (25⁻) levels, respectively. A 91.5-keV transition is in coincidence with the 264-keV and 345-keV transitions. We have assigned this as an additional decay path out of the band to a 6⁺ state which subsequently decays both to the yrast and to the γ band. A similar situation occurs in ¹⁸⁰Os, where the 1928-keV 7⁻ level decays to a 6⁺ level via a 52-keV transition [15].

E. Bands 5 and 6

A γ -ray spectrum gated on the 316-keV transition in band 5 is illustrated in Fig. 2. Band 5 decays to band 8, to the

ground band, and to the even-spin members of the γ band. The 316-keV gated spectrum clearly shows transitions in band 2, confirming that band 2 does decay into band 5. A 285-keV E2 transition links bands 4 and 5, which establishes the spins and parities for band 5 shown on the level scheme. It was not possible to establish spins and parities for band 6, since multipolarity assignments could not be made for the transitions linking that band with band 5 or the rest of the level scheme. Based on the decay pattern of the low-spin members of bands 5,6 and by comparison to similar bands in ¹⁸⁰Os and ¹⁸⁴Pt, bands 5 and 6 most likely have the same parity and are signature partners (see below).

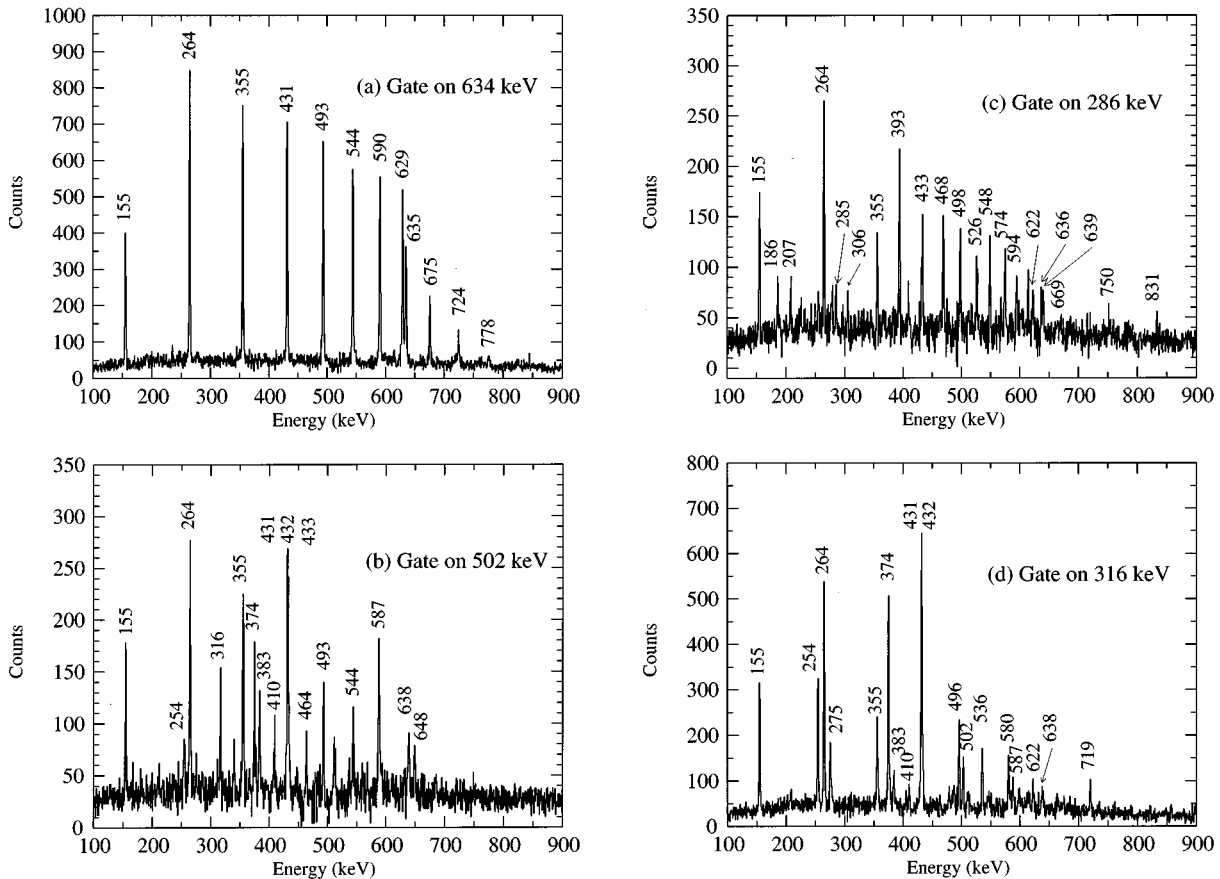


FIG. 2. γ -ray coincidence spectra for selected transitions: (a) γ -634 keV (band 1), (b) γ -502 keV (band 2), (c) γ -286 keV (band 4), and (d) γ -316 keV (band 5). γ -ray energies are labeled in keV.

The 2149-keV level assigned (8^-) in band 6 decays to band 5 and to the γ band via 225-keV and 419-keV transitions, respectively, and the lower-spin state at 1845 keV, assigned (6^-), through a 540-keV transition to the γ band. Note that even though band 6 has many γ rays of similar energies to those in the yrast band, complicating this part of the level scheme, the members of the band are well established by the gates and the energy additivity of the crossing transitions.

F. Band 7

Band 7 is unique in that the strongest transitions associated with it are decays out-of-band to the yrast sequence. The in-band γ rays are seen only weakly. Since none of the transitions connecting band 7 with 1 are clean or intense enough to provide angular distributions, the suggested spin and parity are based on the fact that similar weakly populated bands with strong $\Delta I=2$ and $\Delta I=0$ transitions feeding the yrast band have been observed in ^{184}Pt [12] and ^{180}Os [15,14].

IV. CONFIGURATION ASSIGNMENTS

The experimental aligned angular momenta (i) and routhians (e') are plotted in Figs. 3 and 4 as functions of rotational frequency, following the prescriptions of the cranked shell model (CSM) [22]. Core reference parameters, $J_0=26.5\hbar^2/\text{MeV}$, $J_1=110\hbar^4/\text{MeV}$, were chosen to give a nearly constant alignment in the yrast band following the

crossing observed at $\hbar\omega \approx 0.32$ MeV.

The properties of band 1, which is based on the ground state, will be discussed later. Bands 2–7 in ^{182}Pt are most likely built upon two-quasiparticle configurations, by comparison with theory and with similar bands known in

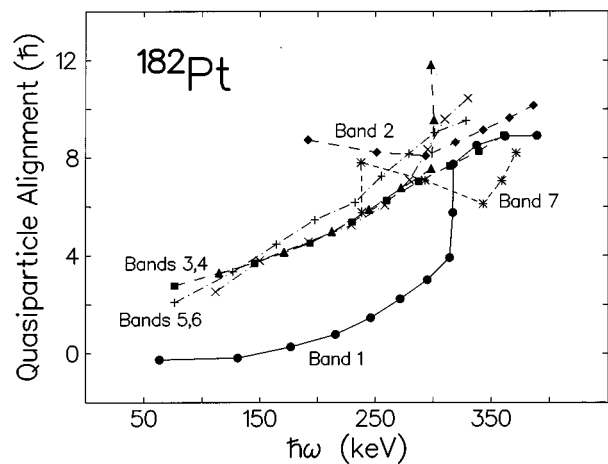


FIG. 3. Quasiparticle aligned angular momenta for the observed bands in ^{182}Pt as a function of rotational frequency. A core reference has been subtracted with the parameters $J_0=26.5\hbar^2/\text{MeV}$, $J_1=110\hbar^4/\text{MeV}$. $K=0$ has been assumed for band 1, $K=1$ for bands 2 and 7, $K=7$ for bands 3 and 4, and $K=5$ for bands 5 and 6 (see text).

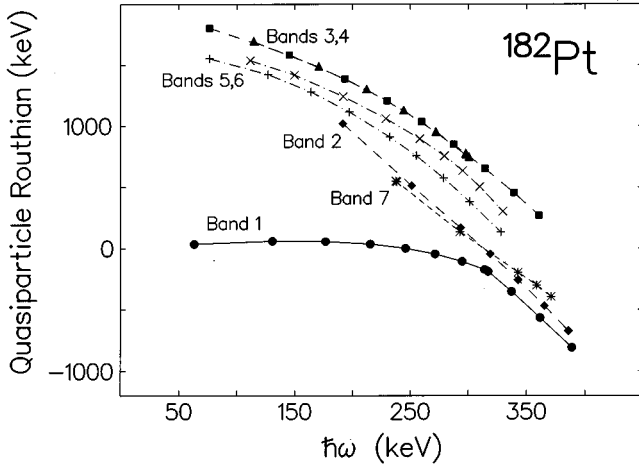


FIG. 4. Quasiparticle Routhians as a function of rotational frequency for the bands observed in ^{182}Pt . A core reference has been subtracted (see previous figure caption).

$^{180,184}\text{Pt}$ [10,12] and ^{180}Os [15], as outlined below. The Nilsson configurations for proton and neutron orbitals lying close to the Fermi surface at $\beta_2 \approx 0.2$, $\omega = 0$ are listed in Table II, along with their spherical-shell-model parentages. A diagram of the single-particle neutron orbital energies as a function of quadrupole deformation may be found in Fig. 3 of Ref. [11]. It should be noted that the neutron positive-parity orbitals, namely, $i_{13/2} 9/2^+ [624]$ and $7/2^+ [633]$, lie very close in energy for $N=104$. As a result of Coriolis- and K -mixing, especially at finite rotational frequency and nonzero γ deformation (see below), it is not clear that one can distinguish between them.

The lowest lying negative-parity neutron orbitals are $1/2^- [521]$, $7/2^- [514]$, and $5/2^- [512]$, arising from the shell-model $p_{3/2}$, $h_{9/2}$, and $f_{7/2}$ configurations, respectively. In principle the $h_{9/2}$ and $f_{7/2}$ configurations can mix but

TABLE II. Quasiparticle configurations and labels for $Z=78$, $N=104$ orbitals close to the Fermi surface at a prolate deformation of $\beta_2 \approx 0.2$. The cranked-shell model labeling follows the commonly used convention set out in Ref. [12].

	Configuration		CSM label	
	Shell model Parentage	Deformed Nilsson	$\alpha = 1/2$	$\alpha = -1/2$
Neutrons	$i_{13/2}$	$9/2^+ [624]^a$	<i>A</i>	<i>B</i>
	$i_{13/2}$	$7/2^+ [633]^a$	<i>C</i>	<i>D</i>
	$f_{7/2}$	$5/2^- [512]$	<i>E</i>	<i>F</i>
	$h_{9/2}$	$7/2^- [514]$	<i>G</i>	<i>H</i>
	$p_{3/2}$	$1/2^- [521]$	<i>E'</i>	<i>F'</i>
Protons	$i_{13/2}$	$1/2^+ [660]$	<i>a</i>	<i>b</i>
	$d_{3/2}$	$3/2^+ [402]$	<i>c</i>	<i>d</i>
	$h_{9/2}$	$1/2^- [541]$	<i>e</i>	<i>f</i>
	$h_{11/2}$	$11/2^- [505]$	<i>g</i>	<i>h</i>
	$h_{11/2}$	$9/2^- [514]$	<i>e'</i>	<i>f'</i>

^aThese two configurations are less than 100 keV apart in the calculation at zero rotational frequency.

TABLE III. Quasiparticle configuration assignments for band structures in ^{182}Pt .

Band	Assignment	(π, α)
1	ground-state band (GSB)	$(+, 0)$
2	$\pi i_{13/2} \otimes h_{9/2}$	$(-, 1)$
3	$\nu i_{13/2} \otimes h_{9/2}$	$(-, 0)$
4	"	$(-, 1)$
5	$\nu i_{13/2} \otimes p_{3/2}$	$(-, 1)$
6	"	$(-, 0)$
7	continuation of GSB ^a	$(+, 0)$
8	oblate band	$(+, 0)$
γ	γ -vibrational band	$(+, 0/1)$

^aAbove spin 18.

Woods-Saxon calculations suggest that at deformations $\beta_2 \approx 0.2$ the negative-parity $K=7/2$ and $K=5/2$ orbitals are fairly pure.

Configuration assignments for bands 2–7 are given in Table III. As discussed below, they are based on a comparison of their spin, parity, $B(M1)/B(E2)$ ratios (bands 3,4) and alignment properties with theory, and with the properties of similar bands in nearby nuclei.

A. Band 2

Band 2 has a high degree of alignment at low frequency ($i \approx 8\hbar$ at $\hbar\omega = 0.2$ MeV) and there is no evidence for a signature partner. In these respects it is similar to band 7 (see below), but differs from band 7 in that band-2 states clearly interact with states in band 5 (see also below). The only combination of quasiparticles which can result in a band with these characteristics is the two-quasiproton configuration $\pi h_{9/2} \otimes i_{13/2}$. This configuration has been assigned to bands with very similar characteristics in ^{184}Pt [12] and ^{186}Pt [23]. The parity and signature shown in Fig. 1 are consistent with this assignment.

B. Bands 3 and 4

Bands 3 and 4 have a modest alignment, $i \approx 4\hbar$ at $\hbar\omega \sim 0.2$ MeV, and negligible energy splitting between the two signatures at low frequency ($\hbar\omega < 0.3$ MeV). Together with the assigned spin and parity of the bandhead state and the negative mixing-ratio (δ) values, these characteristics suggest a two-quasineutron configuration, either $\nu i_{13/2} \otimes h_{9/2}$ or $\nu i_{13/2} \otimes f_{7/2}$. Another possibility is the two-quasiproton configuration $h_{11/2} \otimes h_{9/2}$, which also has negligible signature splitting, but based on systematics it lies several hundreds of keV higher in energy than the two-quasineutron configurations. In addition, the sign of δ would be positive rather than negative.

Strongly coupled negative-parity bands have been observed in ^{184}Pt [12] and assigned as signature partners of the $\nu 9/2^+ [624] \otimes 7/2^- [514]$ configuration, i.e., $\nu i_{13/2} \otimes h_{9/2}$. In that nucleus the bands are built upon a $K^\pi = 8^-$ state with a 1.1-ms lifetime [17], whereas in ^{182}Pt the bandhead state probably has $K=7$ and, within the limits of our coincidence timing resolution (~ 70 ns), no lifetime is observed. The

situation is thus more readily compared to the isotones ^{180}Os , where the lifetime of a 7^- state at similar excitation energy is 27 ± 5 ns [15,14] and ^{184}Hg , where a bandhead state of suggested spin-parity 7^- has been observed [34] with decay characteristics similar to that observed in the present work.

Apart from the experimental limitations, the absence of a measurable lifetime in ^{182}Pt is likely caused by two factors. First, the combination of odd spin and higher excitation energy for the bandhead state in ^{182}Pt opens up a number of possible decay paths to the ground state and other bands. Second, the ^{182}Pt negative-parity bands 3–6 lie closer in energy than their analogues in ^{184}Pt , which could result in some mixing. This would explain the 285-keV $E2$ transition between the band-4 7^- and band-5 5^- states, which would normally be ill favored by the availability of alternative decay paths through $E1$ transitions. Such mixing would be stronger near the bandheads, where states of the same spin parity lie closest in energy. The lower K -value in ^{182}Pt vs ^{184}Pt can be associated with the decrease from $N=106-104$, which brings the $\nu 7/2^+[633]$ orbital closer to the Fermi surface. Based on the modest intensity of the $\Delta I=1$ $M1/E2$ transitions (see below), we suggest that bands 3,4 have a $\nu i_{13/2} \otimes h_{9/2}$ configuration. Given the most probable bandhead-state K value of 7, this corresponds to the Nilsson configuration $7/2^+[633] \otimes 7/2^-[514]$, although as we have said earlier the distinction between $K=7/2$ and $K=9/2$ members of the neutron $i_{13/2}$ family of orbitals is not clear at $N=104$.

C. Bands 5 and 6

Although the spectroscopic data alone do not permit a firm parity assignment for band 6, the presence of similar bands in $^{180,184}\text{Pt}$ and ^{180}Os [14] strongly suggests that bands 5 and 6 are negative-parity signature partners. Likely configurations are $K=4,5$ $\nu i_{13/2} \otimes p_{3/2}$ and $K=7,8$ $\nu i_{13/2} \otimes f_{7/2}$. The two signatures of the $1/2^- [521]$ $\nu p_{3/2}$ orbital lie far apart in energy, as revealed in $^{181,183}\text{Pt}$ [9,11], so that the $\nu i_{13/2} \otimes p_{3/2}$ configuration in ^{182}Pt is expected to possess the same modest degree of signature splitting as the $\nu i_{13/2}$ bands in the neighboring odd- N nuclei. The alternative configuration, $\nu i_{13/2} \otimes f_{7/2}$, is expected to display the same lack of signature splitting as the one-quasineutron $5/2^- [512]$ $\nu f_{5/2}$ configuration in ^{181}Pt . The measured signature splitting of bands 5 and 6, $\Delta e' = 90$ keV at $\hbar\omega = 0.25$ MeV, reflects fairly closely the splitting of the $\nu i_{13/2}$ band in ^{181}Pt , $\Delta e' = 105$ keV [9], favoring the $\nu i_{13/2} \otimes p_{3/2}$ assignment. With this assignment the order of the Routhians for bands 3–6 (see Fig. 4), and the lack of evidence for a strongly coupled band associated with the $\nu i_{13/2} \otimes f_{7/2}$ configuration, are consistent with the order of the Routhians observed in ^{181}Pt [9].

D. Band 7

Band 7 has an alignment of approximately $8\hbar$ at $\hbar\omega = 0.25$ MeV and decays only into the ground-state band, in the spin range $20 \geq I \geq 10\hbar$. Similar bands with positive parity and even spins have been observed in, among others, $^{180,182}\text{Os}$ and $^{180,184,186}\text{Pt}$ nuclei. A wide variety of explana-

tions including prolate multi-quasineutron [10,12,15,24], tilted-axis-cranking (TAC) [25,16], oblate [23], and γ -vibrational [26,27] configurations have been suggested. The assignment of band 7 as the high-spin continuation of the γ band is energetically possible in ^{182}Pt , as is the possibility that band 7 is a continuation of band 8, the oblate structure. Since the γ band has considerable signature splitting at low spin and the odd-spin members are not fed by transitions between the two signatures, it is possible that the odd-spin members would not be observed at high spin. For an oblate rotational band no signature-partner band would be expected. In either case, oblate or γ vibrational, theory predicts that the configuration at frequencies $\hbar\omega > 0.3$ MeV would include a pair of rotationally aligned $i_{13/2}$ neutrons, i.e., $\gamma \otimes AB$ or AB_{oblate} . Based on the systematic properties of similar bands in $^{180-186}\text{Pt}$ and on comparison with CSM calculations, we suggest that band 7 most likely represents the complement of the yrast band undergoing the transition from ground-state band to s band. The evidence for this interpretation is discussed in more detail further on.

E. Band 8

The 0^+ and 2^+ members of band 8 were previously observed by Husson *et al.* [18] following the β decay of ^{182}Au and were interpreted as the first two members of the so-called β band. Low-spin members of such bands have been identified in the even- A $^{180-186}\text{Pt}$ isotopes. As de Voigt *et al.* point out [10], measured large conversion coefficients for the $2_3^+ - 2_1^+$ transitions in ^{180}Pt point to strong $E0$ admixtures, a possible signature of β -vibrational states.

We suggest a more likely interpretation is that band 8 corresponds to a rotational sequence possessing a different shape than the ground-state band. This could also lead to large $E0$ admixtures in the $I-I$ decays. There is now a good deal of theoretical and experimental evidence supporting prolate-oblate shape coexistence in the Pt region, favoring the interpretation of band 8 as a weakly deformed oblate band with a π 4-hole configuration relative to the Pb closed core (e.g. Ref. [2]). The question of shape coexistence at low spin is discussed in the following section.

V. DISCUSSION

A. Theoretical calculations

Theoretical predictions of the nuclear deformation for various quasiparticle configurations have been obtained from deformation self-consistent calculations of the total Routhian surfaces (TRS), performed with a nonaxial Woods-Saxon potential and parameters described in Ref. [28]. Additional details may also be found in Ref. [12]. Selected surfaces are shown in Fig. 5; the quasiparticle labels are explained in Table II. At a frequency $\hbar\omega = 0.17$ MeV, below the frequencies at which any predicted band crossings occur, the ground-state (“vacuum”) configuration is predicted to have a deformation $\beta_2 = 0.25$, $\gamma = -1^\circ$, $\beta_4 = -0.01$. For the two-quasineutron negative-parity configurations associated with bands 3 and 4, theory predicts a somewhat different shape, $\beta_2 = 0.23$, $\gamma = -9^\circ$, $\beta_4 = -0.02$ at $\hbar\omega = 0.21$ MeV. This shift toward oblate deformation can be attributed to the deformation driving characteristics of the high- j $\nu i_{13/2}$ orbital.

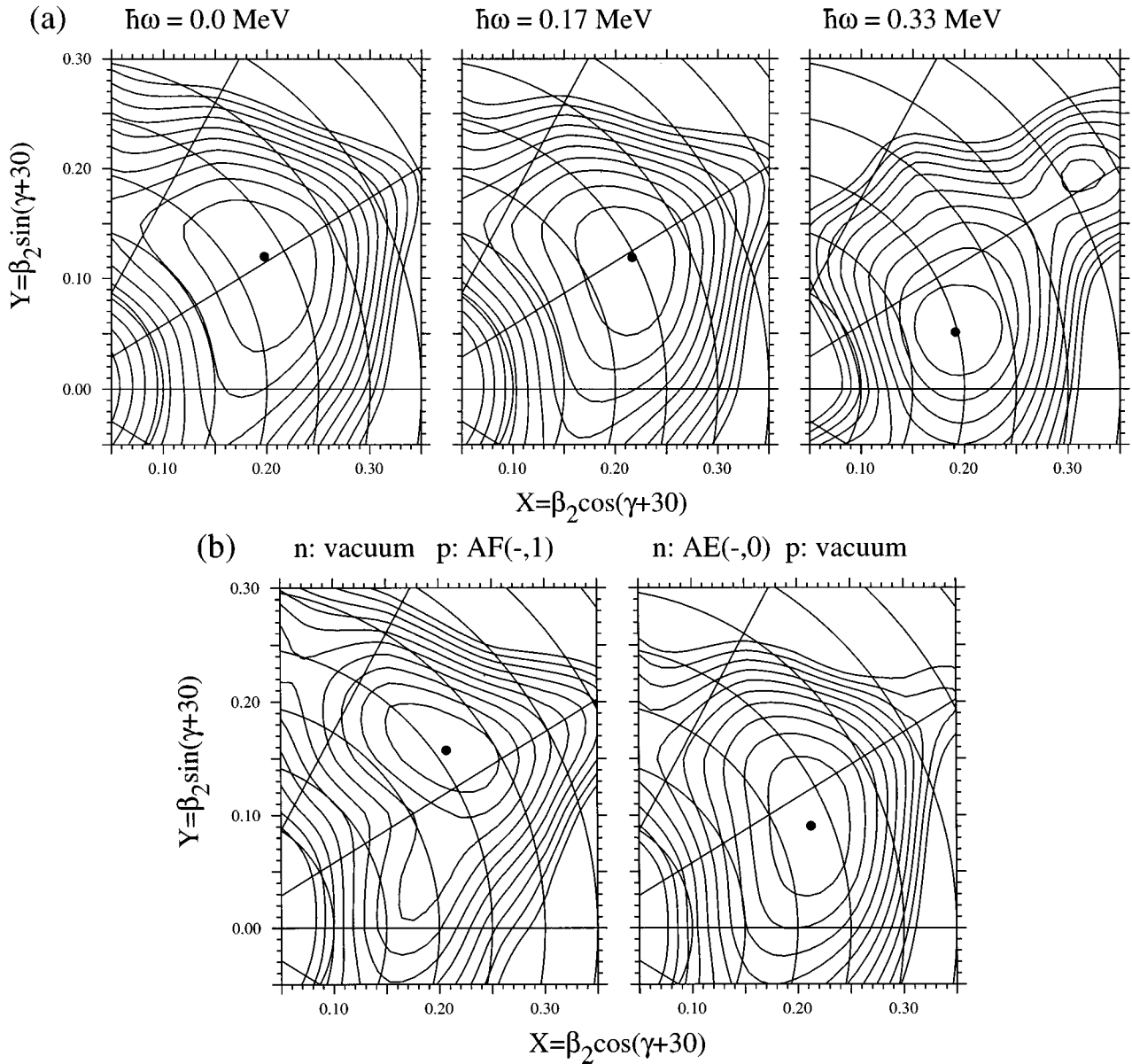


FIG. 5. Theoretical total Routhian surfaces for selected configurations in ^{182}Pt . Details of the calculations are described in Ref. [12]. The quasiparticle labels are given in Table II.

By comparison, theory predicts that the two-quasiproton configuration $\pi i_{13/2} \otimes h_{9/2}$, associated with band 2, possesses a deformation of $\beta_2 = 0.26$, $\gamma = +7^\circ$, $\beta_4 = -0.01$. The positive γ deformation can be attributed to the deformation driving characteristics of the $\pi i_{13/2}$ and $\pi h_{9/2}$ orbitals, both of which have high j and low K .

The TRS results for the ground-state band have been used to calculate the theoretical quasineutron and quasiproton Routhians within the fixed-deformation cranked shell model, as shown in Fig. 6. Figure 7 shows Routhians calculated at a TRS-predicted deformation typical of the two-quasineutron negative-parity configurations. A Woods-Saxon potential and the same prescription as in Ref. [12] have been used. As pointed out by Carpenter *et al.* in their study of ^{184}Pt , there are several close-lying negative-parity neutron orbitals and the calculations do not reproduce precisely the ordering which is observed in the odd- A Pt isotopes. For example, the

$\nu p_{3/2} 1/2^- [521]$ orbital is predicted to lie higher than either of the $\nu h_{9/2} 7/2^- [514]$ or $\nu f_{7/2} 5/2^- [512]$ orbitals, whereas it is the lowest negative-parity sequence observed in $^{181,183}\text{Pt}$ [9,11]. It is, therefore, not surprising that in ^{182}Pt bands 5 and 6 ($\nu i_{13/2} \otimes p_{3/2}$) lie lower in energy than bands 3 and 4 ($\nu i_{13/2} \otimes h_{9/2}$), in disagreement with theory.

The measured energy splitting between the two signature-partner bands 5 and 6 closely resembles the $\nu i_{13/2}$ signature splitting in ^{181}Pt . The magnitude of this splitting is not reproduced by the CSM calculations at $\gamma = 0^\circ$ shown in Fig. 6. Carpenter *et al.* [12] suggest that the deformations of bands which include an $i_{13/2}$ neutron shift toward negative γ values even at fairly low frequency, reaching a γ value of about -10° to -15° just before the first band crossing. Figure 7 shows the calculated quasineutron Routhians for $\gamma = -10^\circ$. Such a deformation increases the energy splitting between the two signatures of the $i_{13/2}$ orbital to $\Delta e' = 90 \text{ keV}$ at

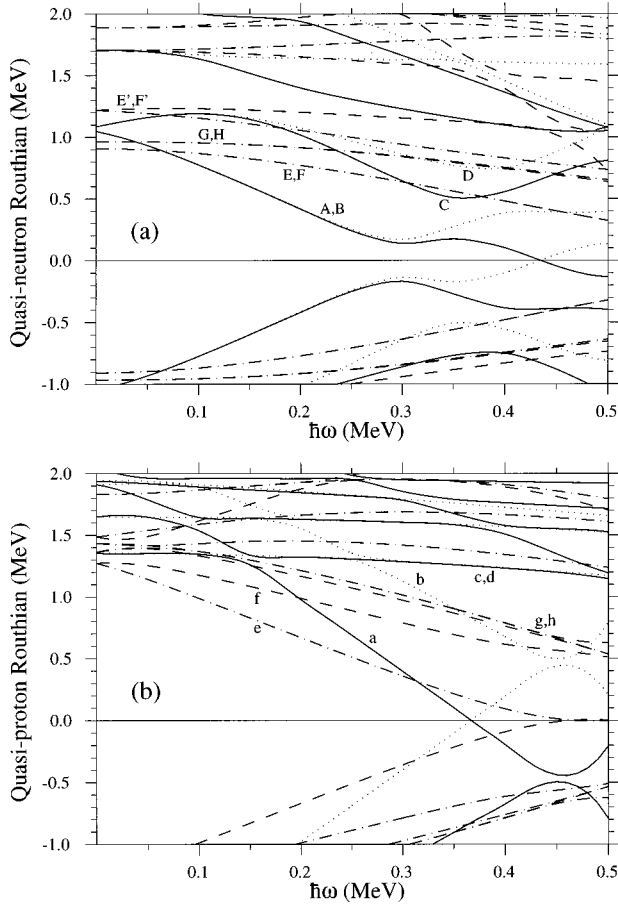


FIG. 6. Theoretical one-quasiparticle Routhians as a function of rotational frequency for (a) $N=104$ and (b) $Z=78$. The deformation parameters used are taken from the TRS results for the ground-state sequence at $\hbar\omega=0.17$ MeV. The Woods-Saxon potential parameters are the same as in Ref. [12]. The neutron and proton pairing are fixed at the so-called BCS values calculated at $\omega=0$.

$\hbar\omega=0.2$ MeV, in agreement with the measured value. A smaller effect is expected for other low-lying neutron orbitals. For example, the calculations of Fig. 7 predict $\Delta e' = 15-20$ keV for the negative-parity configuration associated with bands 3 and 4, while experiment shows an even smaller value, $\Delta e' < 5$ keV.

B. $B(M1)/B(E2)$ ratios for bands 3 and 4

$B(M1; I \rightarrow I-1)/B(E2; I \rightarrow I-2)$ ratios have been extracted from the measured γ -ray branching ratios in the usual manner (e.g., Refs. [15,29]) and are shown in Fig. 8. These are compared to theoretical $M1$ transition matrix elements calculated within the geometrical framework of Dönau and Frauendorf [30], extended to multi-quasiparticle configurations [29], whereby

$$\begin{aligned}
 B(M1; I \rightarrow I-1) = & (3/8\pi I^2) \{ \sqrt{I^2 - K^2} [(g_1 - g_R)K_1 \\
 & + (g_2 - g_R)K_2 + (g_3 - g_R)K_3 + \dots] \\
 & - K[(g_1 - g_R)i_1 + (g_2 - g_R)i_2 \\
 & + (g_3 - g_R)i_3 + \dots] \}^2 \mu_N^2, \quad (1)
 \end{aligned}$$

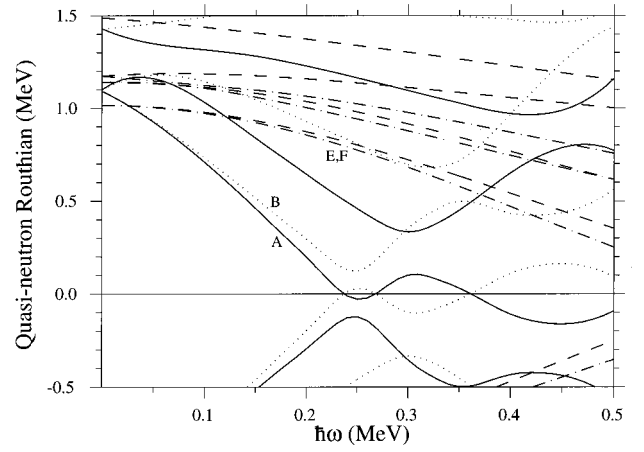


FIG. 7. Theoretical quasineutron Routhians, as in Fig. 6 but for deformation parameters representative of the negative-parity two-quasineutron configurations below any band crossings, according to the TRS calculations (see text).

where

$$K = K_1 + K_2 + K_3 + \dots \quad (2)$$

Parameters for various two-quasiparticle configurations are given in Table IV. The magnetic g_K factors were taken from a Woods-Saxon calculation at $\beta_2=0.23$, $\beta_4=-0.02$. As in Ref. [8], a value of $g_R=0.35$ was used for the core g factor. This value is intermediate to the two other commonly used values, namely $g_R \approx 0.27$ [16] and $g_R = Z/A = 0.43$. Of the observed alignment, $4\hbar$ at $\hbar\omega=0.2$ MeV, half was assigned to each quasiparticle. The $B(E2; I \rightarrow I-2)$ values were calculated by assuming a rotational model and a constant transition quadrupole moment of $Q_0 = 7.1eb$, the experimental value for the ground-state band above spin 6 [38]. As shown in Fig. 8, the measured transition strength ratios are in good

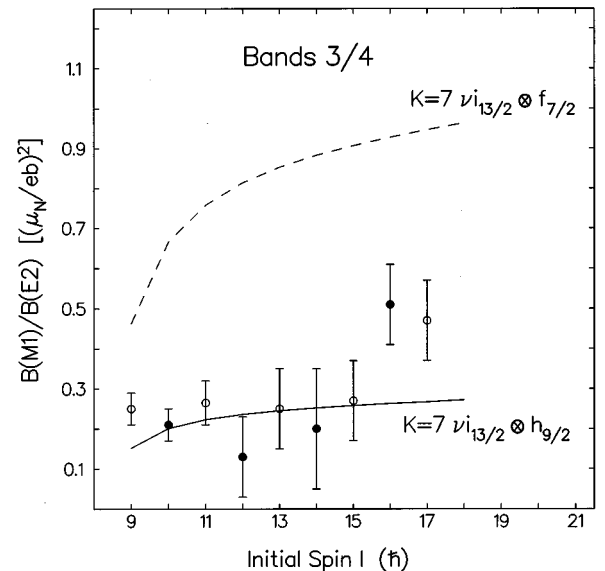


FIG. 8. $B(M1; I \rightarrow I-1)/B(E2; I \rightarrow I-2)$ values for bands 3 and 4. See text for details.

TABLE IV. Parameters used to calculate theoretical $B(M1)$ values for bands 3 and 4 and resulting $B(M1)/B(E2)$ values at spin $I=13\hbar$.

Quasiparticle Configuration	Nilsson Configuration	K	g_1	g_2	$B(M1)/B(E2)$ (μ_N^2/e^2b^2) at $I=13\hbar$
$\nu i_{13/2} \otimes f_{7/2}$	$\nu 9/2^+[624] \otimes 5/2^- [512]$	7	-0.25	-0.41	0.85
"	$\nu 7/2^+[633] \otimes 5/2^- [512]$	6	-0.28	-0.41	0.65
$\nu i_{13/2} \otimes h_{9/2}$	$\nu 9/2^+[624] \otimes 7/2^- [514]$	8	-0.25	0.29	0.44
"	$\nu 7/2^+[633] \otimes 7/2^- [514]$	7	-0.28	0.29	0.25
$\pi h_{11/2} \otimes d_{3/2}$	$\pi 11/2^- [505] \otimes 3/2^+ [402]$	7	1.26	0.11	1.49
"	$\pi 9/2^- [514] \otimes 3/2^+ [402]$	6	1.31	0.11	0.94

agreement with theoretical predictions for the two-quasineutron $\nu i_{13/2} \otimes h_{9/2}$ configuration which has been assigned to these bands.

C. Shape Coexistence at Low Spin

Dracoulis *et al.* [2] have suggested that the low-spin pattern of yrast states in the $^{176-188}\text{Pt}$ isotopes reflects the coexistence of two configurations with different deformations, as originally predicted by Wood [1]. In this picture, the 0_2^+ state in ^{182}Pt represents the (perturbed) bandhead of a weakly deformed oblate ($\beta_2 \approx -0.15$) rotational band having a ‘‘normal’’ four-proton-hole configuration (with respect to ^{186}Pb), coexisting with a well-deformed prolate ($\beta_2 \approx 0.25$) ‘‘intruder’’ band based on the two-particle-six-hole ground state. Subsequently, potential-energy-surface calculations predicted [4,5] that prolate-oblate shape coexistence at low spin is a general feature of this mass region. At $N=104$, neutron midshell, the 0^+ prolate ‘‘intruder’’ band-

head lies well above the ground state in ^{186}Pb [31,32] and $^{184}_{80}\text{Hg}$ [33,34], whereas it becomes the ground state in $^{182}_{78}\text{Pt}$, 490 keV below the oblate bandhead. The energy difference observed in ^{182}Pt is in reasonable agreement with the results of TRS calculations, which predict a prolate-oblate energy difference of 650 keV at zero rotational frequency (Fig. 5). The low-spin features of the $N=104$ band structures are shown in Fig. 9. Apart from perturbations at low spin, caused by interactions between close-lying states [2] (see below), the energy spacings of the bands which are yrast above spin 4 are quite similar, consistent with the suggestion that these bands have similar ‘‘intruder’’ configurations.

The onset of collectivity and related shape-coexistence properties have been studied extensively, especially close to proton closed shells (e.g., Ref. [6]). In particular, Dracoulis has noted [35] that some of the low-spin properties of intruder bands in the Os-Pt-Hg-Pb region may be reproduced in a simple way by considering separate neutron and proton

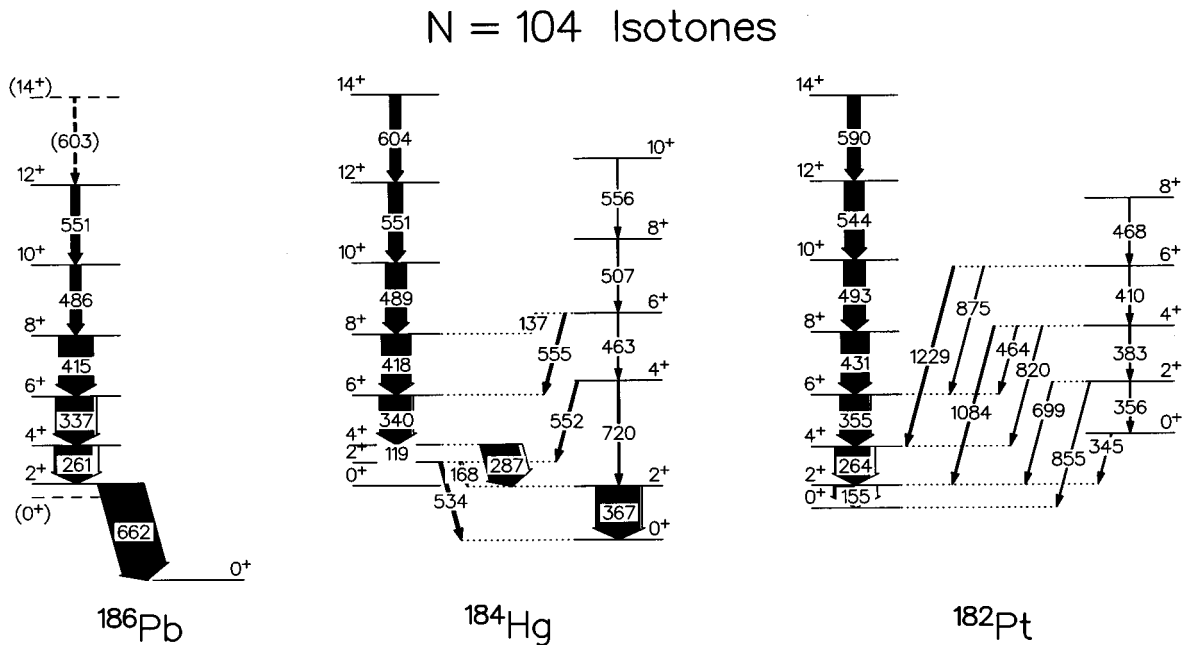


FIG. 9. Coexisting band structures at low spin for even-even $N=104$ isotones close to the $Z=82$ closed shell. ‘‘Intruder’’ bands are shown on the left (prolate deformation), ‘‘normal’’ bands on the right (spherical in Pb, oblate deformation in Hg and Pt). The data are taken from the present work and Refs. [33,34] (^{184}Hg) and [32] (^{186}Pb). The schemes are offset so that the prolate 8^+ states line up.

shells which interact via a quadrupole neutron-proton force acting between pairs of particles (or, equivalently, pairs of holes). In this two-component approach, originally suggested by Heyde and Sau [36], the $2^+ - 0^+$ energy spacings are governed by the shell filling, giving rise to a simple dependence on the number of pairs of valence particles (or holes). The model also predicts coexisting $J^\pi = 2^+$ states which are mixed as a result of the neutron-proton interaction, with an interaction strength given by

$$V = -\frac{\kappa F}{2J+1} \left\{ [N_p N_n] \left(1 - \frac{N_p}{\Omega_p} \right) \left(1 - \frac{N_n}{\Omega_n} \right) \right\}^{1/2}, \quad (3)$$

where κ is the strength of the neutron-proton interaction, which varies little with neutron and proton number, F depends on shell-model radial matrix elements and is taken to be constant for a given major shell, and Ω_n and Ω_p are the shell degeneracies for neutron and proton pairs, respectively. This approach is related to the so-called $N_p N_n$ scheme of Casten and Zamfir [37], whereby low-spin observables can be simply related to the product of numbers of valence neutron and proton pairs. Note that because the model is constructed within a shell-model seniority framework, the interaction between states in a given nucleus is spin dependent.

With the assumption of coexisting oblate and prolate bands, Dracoulis *et al.* [2] have analyzed yrast and yrare excitation energies at low spin for even-even $^{176-184}\text{Pt}$ and extracted a spin-independent interaction strength of $|V| \approx 200$ keV. This value is practically constant as a function of neutron number (see Fig. 10) and for ^{182}Pt is consistent with recent lifetime measurements by Walpe *et al.* [38], which show an $\approx 20\%$ drop in the transition quadrupole moment for the yrast band below spin $6\hbar$, attributable to the strong mixing between states brought on by the interaction. Interaction strengths have also been extracted by Dracoulis and co-workers for Pb and Hg [35] and Os [39] nuclei near neutron midshell; the values for $N=104$ nuclei are shown in Fig. 10.

We choose to compare these values to a modified version of Eq. (3), in which the model dependence on neutron and proton number of pairs is retained while the spin dependence, which arises from specific shell-model assumptions concerning angular-momentum coupling, is not:

$$V_{s-i} = -\kappa' F' \left\{ [N_p N_n] \left(1 - \frac{N_p}{\Omega_p} \right) \left(1 - \frac{N_n}{\Omega_n} \right) \right\}^{1/2}. \quad (4)$$

The value of $\kappa' F' = 0.070$ MeV was chosen to best reproduce the extracted interaction strengths for the $N=100-108$ Pt isotopes and the Os–Pb $N=104$ isotones. The proton- and neutron-pair shell degeneracies were taken from the major-shell structure, i.e., $\Omega_p = (82-50)/2 = 16$ and $\Omega_n = (126-82)/2 = 22$, respectively. For each nucleus, the number of proton pairs was taken from the “normal” configuration; the number of neutron pairs is the same in “normal” and “intruder” configurations in all of these cases. For example, $N_p = 2$ and $N_n = 11$ were used for ^{182}Pt . Using “intruder” values or an average of “intruder” and “normal” values for proton-pair counting results in somewhat different best-fit parameters but the overall results are similar.

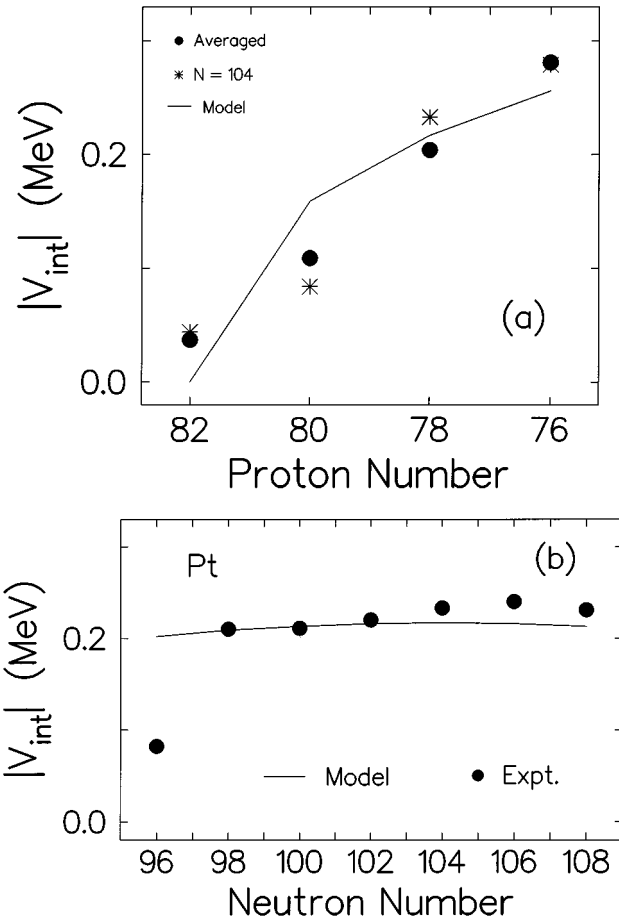


FIG. 10. Interaction strengths for coexisting band structures in $N \approx 104$ nuclei as a function of proton number (a) and in the Pt isotopes as a function of neutron number (b). The experimentally deduced values are taken from the work of Dracoulis and co-workers, viz., [35] (Pb and Hg isotopes), [2] (Pt isotopes), and [39] (Os isotopes). In panel (a), values for the $N=104$ isotones are shown as asterisks while values averaged over $N \approx 104$ nuclei in each isotopic chain are shown as filled circles.

As shown in Fig. 10, with the chosen parameters the agreement between experiment and Eq. (4) is reasonably good. These results suggest that the general picture implied by such a model, that of coexisting structures having different particle-hole configurations relative to the proton closed core, with the interaction-strength properties closely related to the numbers of proton and neutron particles (and holes), is appropriate for these nuclei. It would be interesting to see if more microscopic approaches can reproduce the extracted interaction strengths, as they are potentially sensitive indicators of the detailed structure of these states.

D. γ -vibrational states

The γ band is observed to 7^+ and exhibits a clear staggering between the odd-spin and even-spin members. The phase of the staggering is consistent with a potential energy surface which is fairly flat with respect to γ deformation but minimized for a prolate shape [40–42]. This is in general agreement with the total-Routhian-surface calculations, which predict that the $N \leq 112$ Pt isotopes are γ soft at low

spin [4]. Other theoretical approaches, for example, the dynamic deformation model [5], also predict energy-surface minima for these nuclei which are relatively flat in the γ degree of freedom, compared to nuclei having lower Z . Calculated zero-point energies for the $A \sim 180$ Pt isotopes are typically 1.0–1.2 MeV [40], significantly larger than the energy lost or gained when traversing the γ plane. In this situation the (static) shapes at low spin are not well defined and low-lying γ -vibrational states are expected. This is borne out by the systematic trend in excitation energies of the γ band, which for the $N=104$ Yb–Pt series of isotones gradually decreases with increasing proton number, falling from 1634 keV in ^{174}Yb to its lowest point in ^{182}Pt ; $E(2_3^+) = 667$ keV, within 250 keV of the ground-state band 4^+ energy. Note that $E(2_\gamma^+) \approx E(4_{\text{gsb}}^+)$, and $E(3_\gamma^+) \approx E(4_\gamma^+)$ (see below), are normally associated with a perfectly γ -soft rotor.

The interplay of γ softness and triaxiality in nuclei has been investigated by a number of workers, including Casten *et al.* [42] who addressed the issue of the energy staggering between odd- and even-spin members of the γ bands in Xe and Ba nuclei. Their method incorporates triaxial degrees of freedom within the interacting-boson-approximation (IBA) model, by adding a cubic interaction term to the IBA $O(6)$ -limit Hamiltonian. Energies of excited states and γ -ray branching ratios are determined by two $O(6)$ -Hamiltonian parameters, often denoted B and C , and an additional parameter θ/B which is associated with the degree of γ softness. In terms of level energies, the value of θ/B affects primarily the above-mentioned odd-even staggering in the γ band.

The odd-even staggering in ^{182}Pt is best fit by $\theta/B = 0.34$, with values of B and C determined by fitting the low-spin states in the ground-state band to the $O(6)$ -limit analytical expression. This value of θ/B can be compared to zero in the perfectly γ -soft $O(6)$ limit and to 0.86 for ^{128}Xe , a nucleus which also exhibits an odd-even staggering and has been described as a γ -soft $O(6)$ -like nucleus. Based on the results of Casten *et al.* [42], $\theta/B = 0.34$ corresponds to an approximately 350-keV deep minimum in the potential energy for ^{182}Pt as a function of γ deformation. Compared to the $O(6)$ limit, it also leads to a slight reduction in the calculated fluctuations in γ , from $\gamma_{\text{rms}} = (\langle \gamma^2 \rangle - \langle \gamma \rangle^2)^{1/2} \approx 13\text{--}15^\circ$ to $12\text{--}14^\circ$. It should be noted that these results are not directly comparable to those from the geometric TRS approach. For example, the $O(6)$ -based method, by construction, leads to a potential with a symmetric minimum at a triaxial shape ($\gamma = 30^\circ$), whereas the TRS calculation described in Sec. V A leads to a potential with local minima at prolate and oblate shapes ($\gamma \approx 0^\circ$ and $\pm 60^\circ$, respectively, at zero rotational frequency). Nevertheless, it is clear that in the $O(6)$ -like model the γ -band energy staggering in ^{182}Pt leads to it being placed in the same category as nuclei such as ^{128}Xe , and thus described as very γ soft at low spin.

E. Band crossings at high spin

As shown in Fig. 6, the rotation alignment of a pair of $\nu i_{13/2}$ quasineutrons is predicted to occur at $\hbar\omega \approx 0.30$ MeV. The sharp rise in alignment for band 1 at $\hbar\omega = 0.32$ MeV (see Fig. 3) can be attributed to this band crossing. The possibility of a $\pi h_{9/2}$ crossing at $\hbar\omega < 0.4$ MeV has been raised

in $^{184,185,186}\text{Pt}$ [12,8,23] but generally not accepted as reasonable in the $A < 184$ Pt isotopes (see Ref. [11], for example).

The other sharp increase in alignment observed at $\hbar\omega \approx 0.3$ MeV in ^{182}Pt occurs in band 3. This band is assigned as one signature partner of the $\nu i_{13/2} \otimes h_{9/2}$ configuration, which, since it includes an $i_{13/2}$ neutron, blocks the usual νAB crossing. A γ deformation of -10° , though, as suggested by the TRS calculations, reduces the predicted νBC crossing frequency to $\hbar\omega \approx 0.32$ MeV, matching that seen in experiment. Nevertheless, there is no such alignment gain in band 4, the signature partner to band 3, below $\hbar\omega \approx 0.37$ MeV. The situation may be similar to that observed for a similar two-quasineutron configuration in ^{182}Os bands 2 and 3, where one signature partner undergoes a crossing at $\hbar\omega \approx 0.28$ MeV, while the crossing in the other signature partner is delayed by $\Delta\hbar\omega \approx 0.08$ MeV [16]. In that case no explanation was found.

Band 2 in ^{182}Pt has been assigned a two-quasiproton configuration and therefore one expects to observe a neutron $i_{13/2}$ crossing similar to that observed in the ground-state band. It could be argued that the absence of a large alignment gain in Fig. 3 favors a two-quasineutron assignment involving the neutron $i_{13/2}$ orbital. However, as mentioned earlier, no such configuration can account for the lack of a signature partner and the high alignment at low frequency. It is possible that the modest increase in aligned spin for band 2 at $\hbar\omega > 0.3$ MeV represents the gradual alignment of $i_{13/2}$ neutrons, especially if a different reference were chosen to make the alignment for this band constant at low frequency. This would not change the gradual nature of the increase, though, which is at odds with the sharp increases observed both in the ^{182}Pt ground-state band and in the analogous ^{184}Pt two-quasiproton band. There is therefore no obvious explanation for the observed alignment features above $\hbar\omega = 0.3$ MeV in band 2.

F. Band 7: yrast-yrare interactions at high spin

Band 7 and its analogues in nearby nuclei have been subject to several interpretations. A $(\nu i_{13/2})^2 BC$ configuration has been suggested in the isotone ^{180}Os [15]. In ^{182}Os , two different scenarios have been proposed: (i) a neutron BC configuration, as just mentioned [24] and (ii) a continuation of the positive-signature branch of the γ band [26]. Carpenter *et al.* suggest [12] that at higher frequencies an analogous band in ^{184}Pt may be composed of a mixture of the lowest two- and four-quasiparticle configurations within the $\nu i_{13/2}$ shell, thus involving both the $K=9/2$ (A, B) and the $K=7/2$ (C, D) orbitals. There are selected cases where similar mixed combinations of high- j orbitals have been considered, e.g., ^{86}Zr ($\pi g_{9/2}^n$, mixed $K=3/2, 5/2$) [43] and ^{108}Cd ($\nu g_{9/2}^n$, mixed $K=7/2, 9/2$) [44]. In these instances, however, alternative interpretations were scarce and firm conclusions were not drawn.

Recently, Kutsarova *et al.* [16] have suggested yet another possibility; that in ^{180}Os the BC scenario would give rise to a so-called “ t band” at low rotational frequency ($\hbar\omega \leq 0.2$ MeV), arising from rotation about a tilted axis. In both ^{180}Os and ^{182}Os , though, an accompanying band with positive parity and odd spins has been observed, which lies slightly lower in energy than the even-spin band and has

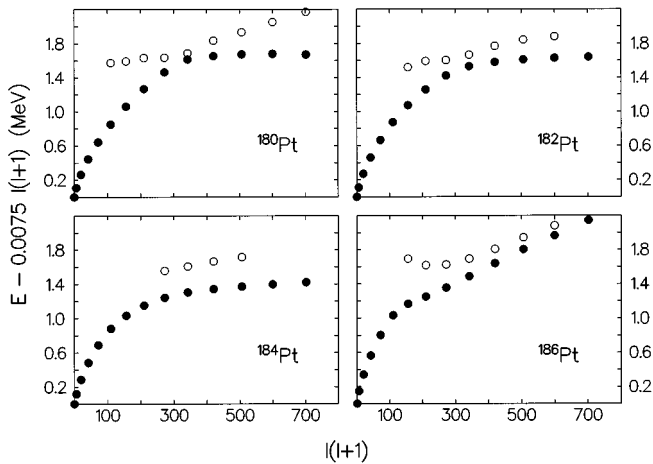


FIG. 11. Excitation energies of the yrast and yrare positive-parity even-spin bands, relative to a rigid-rotor reference, in ^{180}Pt [9], ^{182}Pt (present work), ^{184}Pt [12], and ^{186}Pt [23].

moderately strong $M1/E2$ transitions connecting odd- and even-spin states. This is consistent with CSM calculations (cf., Fig. 6), which predict coupled AC and BC bands which have modest signature splitting and connecting $M1/E2$ transitions. Both the degree of signature splitting and the $B(M1)/B(E2)$ ratios would be similar to those observed in the coupled A, B bands in neighboring odd- N isotopes. In the case of ^{182}Pt , however, no odd-spin partner band has been found, making a BC assignment for band 7 unlikely.

A different explanation has been put forward in the case of ^{186}Pt , where Hebbinghaus *et al.* have suggested [23] that prolate and oblate structures coexist at *high spin*. Subsequent studies showed this to be an unlikely explanation for yrast or near-yrast bands in lighter Pt isotopes, e.g., ^{184}Pt [12], supported by TRS calculations which predict that close to neutron midshell oblate structures rapidly become nonyrast with increasing rotational frequency and spin.

In ^{180}Pt the two positive-parity even-spin bands coexist over the spin range 12^+ to 26^+ , which has been interpreted as an extended interaction between the ground-state band and the $\nu i_{13/2}^{2-} AB$ s band [10]. If true, we would expect similar features across the chain of Pt isotopes and expect that the interaction strengths as a function of neutron number would exhibit the characteristic oscillatory pattern seen for $\nu i_{13/2}^{2-}$ crossings in other mass regions [45]. Relative excitation energies of the yrare even-spin, even-parity bands in the Pt nuclei for which published data exist are shown in Fig. 11. To varying degrees these structures all approach the yrast band at moderate spin and, except in the case of ^{186}Pt , are repelled at higher spin. In a two-band extended mixing approach, the interaction strength is at most half the energy gap at closest approach and can be accurately determined if γ -ray intensities for transitions connecting the two branches are known, as is the case for ^{180}Pt . In the absence of branching ratios, which is the case for $^{182,184,186}\text{Pt}$, limits on the interaction strength can be obtained by estimating limits on the unobserved transition intensities. For example, in ^{182}Pt the 825-keV out-of-band and 687-keV in-band transitions de-exciting the 20_2^+ level are observed but are too weak to obtain reliable intensities. Nevertheless, we can estimate that the out-of-band to in-band branching ratio does not exceed

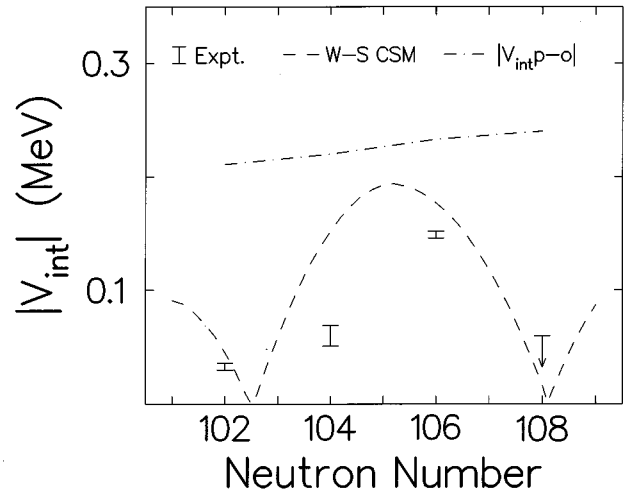


FIG. 12. Interaction strengths between yrast and yrare positive-parity bands at high spin in the Pt isotopes near $N=104$. The experimentally deduced values are discussed in the text. Theoretical predictions for interacting ground-state and $\nu i_{13/2}^{2-} s$ bands were extracted from Woods-Saxon CSM calculations (see caption to Fig. 6). For comparison, interaction strengths for shape-coexisting bands at low spin are shown, as deduced by Dracoulis *et al.* [2].

$\lambda \approx 4$, otherwise the weaker of the two transitions would not have been observed in our experiment.

The results of such an analysis are shown for $^{180-186}\text{Pt}$ in Fig. 12. Theoretical values have been extracted from CSM calculations at fixed deformation, an example of which is shown in Fig. 6. Although some of the experimental values are imprecise it can be seen that they approximate the pattern suggested by theory and they clearly differ from the prolate-oblate interaction values deduced by Dracoulis *et al.* [2]. Therefore, we suggest that these yrare branches represent the complement of the yrast “vacuum” configuration observed over the spin range in which the neutron s band crosses the ground-state band. A similar explanation has been advanced [46] regarding yrare band structures in the odd-proton nuclei ^{175}Re and ^{177}Ir . Such states are expected theoretically [45] but are usually not observed. As mentioned above, it is possible that the explanation for $N \geq 108$ may not be this simple: the two bands in ^{186}Pt converge rapidly up to a certain spin, $I \approx 16$, but above that their trajectories are similar. As discussed by Hebbinghaus *et al.* [23], a change from prolate to oblate shapes in the low-lying states of the Pt isotopes occurs at $N \approx 110$, and it is possible that oblate states influence the high-spin structure at $N=108$ already.

G. Interaction between bands 2 and 5

Interband $E2$ transitions are observed linking (15^-) and (13^-) states in bands 2 and 5. A similar situation occurs in ^{184}Pt [12], where a 6.3-keV interaction strength has been measured between the two close-lying 13^- states. The small value is interpreted as being due to the significant structural differences between the two configurations. A precise value of the mixing in ^{182}Pt cannot be obtained, due to contaminant transitions and the fact that the (15^-) and (13^-) pairs of states both appear to be mixed, lying 63 and 50 keV apart, respectively. Within the standard two-band mixing approach the interaction strength must be less than or equal to half the smallest energy gap between states of like spin and parity,

i.e., $|V_{\text{int}}| \leq 25$ keV. As in ^{184}Pt , it is suggested that bands 5/6 and 3/4 in ^{182}Pt have very different quasiparticle configurations and are expected to interact little.

VI. SUMMARY

The level structure of ^{182}Pt has been studied to high spin with heavy-ion reactions and γ -ray spectroscopic techniques. Nine band structures, seven of which are rotational bands associated with a prolate shape, have been placed in a level scheme which extends to approximately 7 MeV in excitation energy and ($27\hbar$) in spin. Their configurations can be explained by comparison to Woods-Saxon cranked-shell-model calculations, to band structures observed in nearby nuclei and, in the case of the strongly coupled bands 3,4 by their characteristic $B(M1)/B(E2)$ ratios. For even-even nuclei close to ^{182}Pt , the low-spin energy systematics of bands built upon the ground state and the first excited 0^+ state and the interactions between those bands, appear to be well described within a shape coexistence framework involving ‘‘normal’’ proton hole states and ‘‘intruder’’ proton particle-

hole states, relative to the $Z=82$ closed-shell core. At higher spin, a ground-state band crossing at $\hbar\omega \approx 0.32$ MeV has been attributed to the rotational alignment of a pair of $i_{13/2}$ quasineutrons, in agreement with theory. However, it seems difficult to explain the lack of related band crossings in some of the sidebands, notably bands 2 and 4. The characteristics of the rare positive-parity even-spin bands in $^{180,182,184}\text{Pt}$ and possibly ^{186}Pt suggest they represent the complement of the ‘‘vacuum’’ configuration, observed through the ground-state band crossing, i.e., in each case they are the higher-lying branch of two bands interacting with significant strength.

ACKNOWLEDGMENTS

We gratefully acknowledge the assistance of staff at the McMaster University tandem-accelerator laboratory and the Orsay IPN synchrocyclotron laboratory. We also thank J.C. Walpe and U. Garg for the use of their ^{182}Pt lifetime results prior to publication. This work has been supported by the Canadian NSERC, the French IN2P3, and the German BMBF; research at the University of Tennessee is supported by the U.S. DOE under Contract No. DE-FG05-87ER40361.

-
- [1] J.L. Wood, in *Proceedings of the 4th International Conference on Nuclei Far From Stability*, Helsingor, Denmark, 1981, edited by P.G. Hansen and O.B. Nielsen (CERN Report No. 81-09, 1981), p. 612; J.L. Wood, in *Lasers in Nuclear Physics*, Nuclear Science Research Conference Series Vol. 3, edited by C. E. Bemis, Jr. and H. K. Carter (Harwood, New York, 1982), p. 481.
- [2] G.D. Dracoulis, A.E. Stuchbery, A.P. Byrne, A.R. Poletti, S.J. Poletti, J. Gerl, and R.A. Bark, *J. Phys. G* **12**, L97 (1986).
- [3] J. Wauters, N. Bijmens, P. Dendooven, M. Huyse, Han Yull Hwang, G. Reusen, J. von Schwarzenberg, P. Van Duppen and ISOLDE Collaboration, R. Kirchner, and E. Roeckl, *Phys. Rev. Lett.* **72**, 1329 (1994).
- [4] R. Bengtsson, T. Bengtsson, J. Dudek, G. Leander, W. Nazarewicz, and J.-ye Zhang, *Phys. Lett. B* **183**, 1 (1987).
- [5] M. Veskovic, M.K. Harder, K. Kumar, and W.D. Hamilton, *J. Phys. G* **13**, L155 (1987).
- [6] J.L. Wood, K. Heyde, W. Nazarewicz, M. Huyse, and P. Van Duppen, *Phys. Rep.* **215**, 101 (1992).
- [7] A.J. Larabee, M.P. Carpenter, L.L. Riedinger, L.H. Courtney, J.C. Waddington, V.P. Janzen, W. Nazarewicz, J.-Y. Zhang, R. Bengtsson, and G.A. Leander, *Phys. Lett.* **169B**, 21 (1986).
- [8] V.P. Janzen, M.P. Carpenter, L.L. Riedinger, W. Schmitz, S. Pilotte, S. Monaro, D.D. Rajnauth, J.K. Johansson, D.G. Popescu, J.C. Waddington, Y.S. Chen, F. Donau, and P.B. Semmes, *Phys. Rev. Lett.* **61**, 2073 (1988).
- [9] M.J.A. de Voigt, R. Kaczarowski, H.J. Riezebos, R.F. Noorman, J.C. Bacelar, M.A. Deleplanque, R.M. Diamond, and F.S. Stephens, *Nucl. Phys.* **A507**, 447 (1990).
- [10] M.J.A. de Voigt, R. Kaczarowski, H.J. Riezebos, R.F. Noorman, J.C. Bacelar, M.A. Deleplanque, R.M. Diamond, F.S. Stephens, J. Sauvage, and B. Roussi ere, *Nucl. Phys.* **A507**, 472 (1990).
- [11] J. Nyberg, A. Johnson, M.P. Carpenter, C.R. Bingham, L.H. Courtney, V.P. Janzen, S. Juutinen, A.J. Larabee, Z.M. Liu, L.L. Riedinger, C. Baktash, M.L. Hallert, N.R. Johnson, I.Y. Lee, Y. Schutz, J.C. Waddington, and D.G. Popescu, *Nucl. Phys.* **A511**, 92 (1990).
- [12] M.P. Carpenter, C.R. Bingham, L.H. Courtney, V.P. Janzen, A.J. Larabee, Z.-M. Liu, L.L. Riedinger, W. Schmitz, R. Bengtsson, T. Bengtsson, W. Nazarewicz, J.Y. Zhang, J.K. Johansson, D.G. Popescu, J.C. Waddington, C. Baktash, M.L. Halbert, N.R. Johnson, I.Y. Lee, Y.S. Schutz, J. Nyberg, A. Johnson, R. Wyss, J. Dubuc, G. Kajrys, S. Monaro, and S. Pilotte, *Nucl. Phys.* **A513**, 125 (1990).
- [13] V.P. Janzen, Z.M. Liu, M.P. Carpenter, L.H. Courtney, A.J. Larabee, L.L. Riedinger, J.K. Johansson, D.G. Popescu, J.C. Waddington, G. Kajrys, S. Monaro, and S. Pilotte, *Phys. Rev. C* **45**, 613 (1992).
- [14] G.D. Dracoulis, C. Fahlander, and M.P. Fewell, *Nucl. Phys.* **A383**, 119 (1982).
- [15] R.M. Lieder, A. Neskakis, J. Skalski, G. Sletten, J.D. Garrett, and J. Dudek, *Nucl. Phys.* **A476**, 545 (1988).
- [16] T. Kutsarova, R.M. Lieder, H. Schnare, G. Hebbinghaus, D. Balabanski, W. Gast, A. Kr amer-Flecken, M.A. Bentley, P. Fallon, D. Howe, A.R. Mokhtar, J.F. Sharpey-Schafer, P. Walker, P. Chowdhury, B. Fabricius, G. Sletten, and S. Frauendorf, *Nucl. Phys.* **A587**, 111 (1995).
- [17] J. Burde, R.M. Diamond, and F.S. Stephens, *Nucl. Phys.* **A92**, 306 (1967).
- [18] J.P. Husson, R. Foucher, A. Knipper, G. Klotz, G. Walter, C.F. Liang, C. Richard-Serre, and the ISOLDE Collaboration, *Proceedings of the International Conference on Nuclei Far From Stability*, Cargese, Corsica, 1976 (CERN Report No. 76-13, 1976), p. A85.
- [19] M. Cailliau, R. Foucher, J.P. Husson, and J. Letessier, *J. Phys. (France) Suppl. Lett.* **35**, L-233 (1974).
- [20] G. Palameta and J.C. Waddington, *Nucl. Instrum. Methods Phys. Res. A* **234**, 476 (1985).

- [21] R.A. Bark, C. Rossi-Alvarez, G. de Angelis, A. Atac, D. Bazzacco, R. Burch, A. Bracco, F. Camera, G. Hagemann, B. Herskind, W. Korten, S. Leoni, R. Menagazzo, B. Million, D. Napoli, P. Pavan, M. Piganelli, M. Piiparinen, M. de Poli, G. Sletten, P. Spolaore, and J. Wrzesinski, *Laboratori Nazionali di Legnaro dell'INFN 1993 Annual Report*, Legnaro, 1994 (unpublished).
- [22] R. Bengtsson, S. Frauendorf, and F.-R. May, *At. Data Nucl. Data Tables* **35**, 15 (1986), and references therein.
- [23] G. Hebbinghaus, W. Gast, A. Krämer-Flecken, R.M. Lieder, J. Skalski, and W. Urban, *Z. Phys. A* **328**, 387 (1987).
- [24] C. Fahlander and G.D. Dracoulis, *Nucl. Phys.* **A375**, 263 (1982).
- [25] S. Frauendorf, *Nucl. Phys.* **A557**, 259c (1993).
- [26] P. Chowdhury, F. Azgui, S. Bjørnholm, J. Borggreen, C. Christensen, B. Fabricius, A. Holm, J. Pedersen, G. Sletten, M. Bentley, D. Howe, R. Mokhtar, D. Morrison, and J.F. Sharpey-Schafer, *Niels Bohr Institute Tandem Accelerator Laboratory Annual Report*, 1987 (unpublished).
- [27] Y.R. Shimizu, *Proceedings of the Lund Workshop on the $A=180$ Region*, Lund Institute of Technology, 1988 (unpublished).
- [28] W. Nazarewicz, J. Dudek, R. Bengtsson, T. Bengtsson, and I. Ragnarsson, *Nucl. Phys.* **A435**, 397 (1985).
- [29] D.C. Radford, H.R. Andrews, G.C. Ball, D. Horn, D. Ward, F. Banville, S. Flibotte, S. Monaro, S. Pilotte, P. Taras, J.K. Johansson, D. Tucker, J.C. Waddington, M.A. Riley, G.B. Hagemann, and I. Hamamoto, *Nucl. Phys.* **A545**, 665 (1992).
- [30] F. Dönau and S. Frauendorf, in *Proceedings of the Conference on High Angular Momentum Properties of Nuclei*, Oak Ridge, Tennessee, 1982, edited by N.R. Johnson (Harwood Academic, New York, 1983), p. 143; F. Dönau, *Nucl. Phys.* **A471**, 469 (1987).
- [31] J. Heese, K.H. Maier, H. Grawe, J. Grebosz, H. Kluge, W. Meczynski, M. Schramm, R. Schubart, K. Spohr, and J. Styczen, *Phys. Lett. B* **302**, 390 (1993).
- [32] A.M. Baxter, A.P. Byrne, G.D. Dracoulis, R.V.F. Janssens, I.G. Bearden, R.G. Henry, D. Nisius, C.N. Davids, T.L. Khoo, T. Lauritsen, H. Penttillä, D.J. Henderson, and M.P. Carpenter, *Phys. Rev. C* **48**, R2140 (1993).
- [33] W.C. Ma, A.V. Ramayya, J.H. Hamilton, S.J. Robinson, J.D. Cole, E.F. Zganjar, E.H. Spejewski, R. Bengtsson, W. Nazarewicz, and J.-Y. Zhang, *Phys. Lett.* **167B**, 277 (1986).
- [34] J.K. Deng, W.C. Ma, J.H. Hamilton, A.V. Ramayya, J. Kormicki, W.B. Gao, X. Zhao, D.T. Shi, I.Y. Lee, J.D. Garrett, N.R. Johnson, D. Winchell, M. Halbert, and C. Baktash, *Phys. Rev. C* **52**, 595 (1995).
- [35] G.D. Dracoulis, *Phys. Rev. C* **49**, 3324 (1994).
- [36] K. Heyde and J. Sau, *Phys. Rev. C* **33**, 1050 (1986).
- [37] R.F. Casten and N.V. Zamfir, *Phys. Rev. Lett.* **70**, 402 (1993).
- [38] J.C. Walpe (private communication); J.C. Walpe, U. Garg, S. Naguleswaran, W. Reviol, J. Wei, D. Ye, I. Ahmad, I. Bearden, M.P. Carpenter, R.V.F. Janssens, T.L. Khoo, and T. Lauritsen, *Bull. Am. Phys. Soc.* **39**, 1419 (1994).
- [39] T. Kibédi, G.D. Dracoulis, A.P. Byrne, P.M. Davidson, and S. Kuyucak, *Nucl. Phys.* **A567**, 183 (1994).
- [40] K. Kumar and M. Baranger, *Nucl. Phys.* **A110**, 529 (1968).
- [41] J. Meyer-ter-Vehn, *Nucl. Phys.* **A249**, 111 (1975); **A249**, 141 (1975).
- [42] R.F. Casten, P. Von Brentano, K. Heyde, P. Van Isacker, and J. Jolie, *Nucl. Phys.* **A439**, 289 (1985).
- [43] I. Hamamoto, *Proceedings of the First Lanzhou Summer School*, Lanzhou, People's Republic of China (Springer-Verlag, Berlin, 1990); (private communication).
- [44] I. Thorslund, C. Fahlander, J. Nyberg, S. Juutinen, R. Julin, M. Piiparinen, R. Wyss, A. Lampinen, T. Lönnroth, D. Müller, S. Törmänen, and A. Virtanen, *Nucl. Phys.* **A564**, 285 (1993).
- [45] R. Bengtsson and S. Frauendorf, *Nucl. Phys.* **A327**, 139 (1979).
- [46] R.A. Bark, S.W. Ødegård, R. Bengtsson, I.G. Bearden, G.B. Hagemann, B. Herskind, F. Ingebretsen, S. Leoni, H. Ryde, T. Shizuma, K. Strähle, P.O. Tjøm, and J. Wrzesinski, *Phys. Rev. C* **52**, R450 (1995).